J|A|C|S COMMUNICATIONS

Published on Web 02/23/2009

Colloidal Synthesis of Infrared-Emitting Germanium Nanocrystals

Doh C. Lee, Jeffrey M. Pietryga, Istvan Robel, Donald J. Werder, Richard D. Schaller, and Victor I. Klimov*

Chemistry Division, C-PCS, MS-J567, Los Alamos National Laboratory, Los Alamos, New Mexico 87545

Received November 25, 2008; E-mail: klimov@lanl.gov

Nanocrystals (NCs) of group IV semiconductor materials, such as silicon (Si) and germanium (Ge), have been of tremendous fundamental and technological interest since the observation of photoluminescence (PL) from quantum-confined Si.[1] The narrow band gap of bulk Ge (0.67 eV at 300 K) renders Ge NCs particularly interesting as low-toxicity replacements for infrared (IR) III−V and IV−VI lead chalcogenide NCs in applications such as light-emitting diodes and solar cells, and as biolabels at tissue-transparent wavelengths (700−1100 nm). Observations of IR PL from Ge NCs fabricated by physical methods[2,3] are promising, but these methods are expensive and unscalable, and produce matrix- or substrate-bound NCs, which limits the scope of potential application. Colloidal synthesis is an effective methodology for the scalable production of high-quality, solution-processible NCs of numerous semiconductors, especially II−VI,[4] IV−VI,[5] and III−V[6] materials. However, NCs of group IV semiconductors have proven to be much more difficult to synthesize colloidally, which has been attributed to the high crystallization temperatures of these materials due to strong covalent bonding.[7] In fact, among numerous published accounts of colloidal pathways to Ge NCs,[8−14] fine control over size and crystallinity in one step remains difficult, and IR PL has never been observed.

Here, we report the first colloidal synthesis of IR-emitting Ge NCs, with PL quantum yields (QYs) as high as ∼8%. NC diameters ranged from 3.2 ± 0.4 to 6.4 ± 1.9 nm by transmission electron microscopy (TEM, Figure 1A). The PL peak wavelength increased with size from 900 to 1400 nm (Figure 1B), in accord with expectations of quantum confinement effects, although emission from large NCs (>4.5 nm) was much weaker in intensity.

A typical synthesis of 4 nm NCs is described as follows: under inert atmosphere, GeI_2 (0.2 g, 0.6 mmol) is dissolved in hexadecylamine (HDA, 3 g) in a 50-mL three-neck round-bottom flask by heating to 200 °C. *N*-Butyllithium (0.8 mL of a 1.6 M hexane solution) diluted with 3 mL of 1-octadecene (ODE) is then injected, and the reaction mixture is further heated to 300 °C. After 1 h, the heat source is removed and the reaction is allowed to cool. At ∼100 °C, the reaction product is transferred to a centrifuge tube. The NCs are precipitated by adding an equal volume of methanol, and the mixture is centrifuged. After discarding the supernatant, the precipitate is redissolved in a nonpolar solvent (hexane, toluene, or chloroform). Residual HDA is removed by repeating the precipitation/resuspension procedure using a mixture of acetone and methanol 4 times. Larger NCs were produced by increasing the concentrations of all precursors (e.g., 5-fold for 6.4 nm NCs). Interestingly, smaller NCs were produced when the reaction and purification steps were performed under ambient conditions. Regardless of whether this is due to reduced reactivity of the precursors or to an oxygen-driven *in situ* etching, particles in all cases are found to be highly crystalline cubic Ge by a combination of powder X-ray diffraction, energy dispersive X-ray spectroscopy, and high-resolution TEM (Figure 1A inset), with no evidence of residual Ge oxides.

The effects of other reaction variables, including solvents, reducing agents, and capping ligands, on NC stability and PL were also

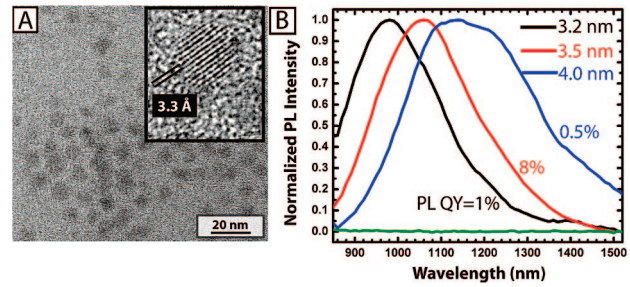

Figure 1. (A) TEM images of Ge NCs (4.0 ± 1.7 nm) whose PL peak centers at 1160 nm (blue curve in Figure 1B). Inset shows high-resolution TEM image of a single Ge NC. The lattice spacing, measured by taking fast Fourier transform of the image, matches the (111) *d*-spacing of cubic Ge. (B) Normalized PL spectra (excited at 808 nm) of ODE-capped Ge NCs at room temperature. Green curve shows PL (not normalized) of TOP-capped Ge NCs (3.8 ± 0.8 nm).

examined. GeI_2 was most readily soluble in HDA; limited solubility ultimately hampered reactions attempted in other solvents [trioctylamine, dioxane, ODE, and trioctylphosphine (TOP)]. Likewise, the use of the poorly soluble reducing agent $LiAlH_4$, instead of the soluble and more reactive *n*-butyllithium, resulted in low-quality NCs with poor solubility. Surprisingly, the addition of ODE as a ligand, rather than as solvent, was found to have the most dramatic effect on the quality of the product NCs. Addition of ODE at 200 °C improved the PL quantum yield of the NCs, relative to, e.g., TOP-capped NCs similar to those published in ref 12 (Figure 1B).

TOP- and ODE-capped NCs also show a significant difference in their susceptibility toward oxidation. This is demonstrated starkly in Figure 2A, in which hexane solutions of TOP- and ODE-capped NCs were stirred in the presence of equal amounts of water. Although germanium is highly sensitive to oxidation upon exposure to air and moisture, the ODE-passivated sample remains distinctly brown, indicating the presence of Ge NCs, for 3−4 weeks until the solution gradually fades to light brown. In contrast, the TOP-capped solution loses all color within 72 h, indicating that the NCs were oxidized into water-soluble germanium oxides.[15,16] In addition, the PL of ODE-capped NCs remained largely unchanged after 72 h of agitation in water, although over longer time periods (∼1 month) a blue shift of up to 100 meV was observed.

The enhanced qualities of ODE-capped Ge NCs can be understood in terms of the effectiveness of organic passivation of the NC surfaces. Strongly bound ligands can confer greater resistance toward oxidation and particle aggregation, and can enhance PL efficiency by saturating chemically undercoordinated "trap" sites. In this study, the enhanced PL and stability are likely due to the formation of strong, covalent Ge−C bonds, evidence of which can be found in the Fourier transform IR (FT-IR) spectra (Figure 2B). The lack of characteristic 1-alkene peaks (at ∼900, ∼1000, ∼1620, and immediately higher than 3000 cm^{-1}) and the appearance of a sharp Ge−C stretch peak at 700 cm^{-1} [17] are indicative of the reaction of ODE with Ge NC surfaces in a manner

10.1021/ja809218s CCC: $40.75

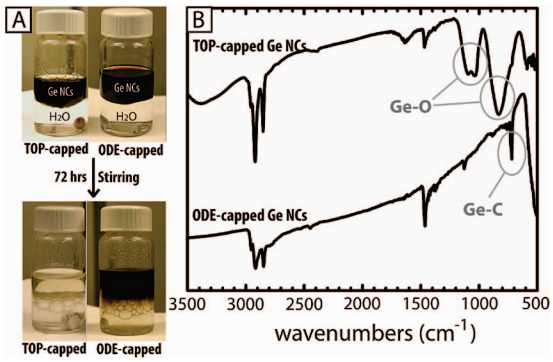

Figure 2. (A) Mixtures of TOP- (left) and ODE-capped (right) Ge NC hexane solutions and water before (top) and after (bottom) 72 h of stirring. The TOP-capped NCs fade to pale yellow after mixing, whereas ODE-capped NCs stay nearly the same color. (B) FT-IR spectra of films from TOP-capped (upper) and ODE-capped (lower) NCs.

similar to that known for 1-alkenes.[18] A similar reaction has been observed between Si NCs and alkenes, yielding strong Si−C bonds which help reduce surface oxidation, enhancing the chemical and optical stability of the NCs.[19,20] Further evidence of the effectiveness of this passivation in Ge NCs can also be found in Figure 2B. After 5 months under ambient conditions, spectra of TOP-capped NCs feature a strong, broad band at 840 cm^{-1} not found for ODE-capped NCs, which can be attributed to Ge−O bonds. This implies that Ge−C bond formation enhances the resistance of Ge NCs toward oxidation.

As with PL, the energy of the absorption onset of these Ge NCs decreases with increasing size (Figure 3A). Further, size selected particles from a single batch also showed predicted behavior: larger NCs that precipitated out first showed lower PL energy than those which remained in supernatant after partial precipitation, as expected. For all samples, PL and absorption onset energy (Figure 3A inset and 3B) were in close proximity, which implies that the emission is likely from the band-edge transition. In fact, the observed size-dependence trend of these features is similar to that produced for quantum-confined particles by a simple particle-in-a-box model, with exact values similar to those predicted by more sophisticated tight-binding calculations[21] (Figure 3B).

A few samples from this study also show weak PL peaks in the visible to UV range (550 to 350 nm) together with IR PL but with QYs typically 1−2 orders of magnitude lower. Several research groups have reported visible luminescence from Ge NCs,[8−10,22−24] which has often been attributed to quantum-confined, band-edge emission. Despite the size dependence of visible PL claimed by some groups,[9,22] the variation in emission wavelength with size across multiple reports, taken as a whole, is very weak. In the present study, we find no consistent size dependence of the occasionally observed visible emission. We suggest that this higher-energy emission, in this and previous studies, is likely due to minor, uncontrolled amounts of luminescent GeO_x species.[25]

In summary, we synthesized the first colloidal Ge nanocrystals exhibiting IR PL. The consistent agreement between the energy of the absorption onset and the PL peak suggests that the IR emission comes from a band-edge transition, in contrast to earlier reports of band-edge emission at much higher energies. We contend that this IR PL is now observable because of the highly effective passivation by ODE, which also stabilizes the NC surfaces against oxidation. We are currently investigating whether the reaction between alkenes and the Ge surface can be enhanced to further improve emission and chemical stability. In addition, studies of carrier dynamics to unveil the origin of PL and the effect of confinement on Ge electronic properties are underway.

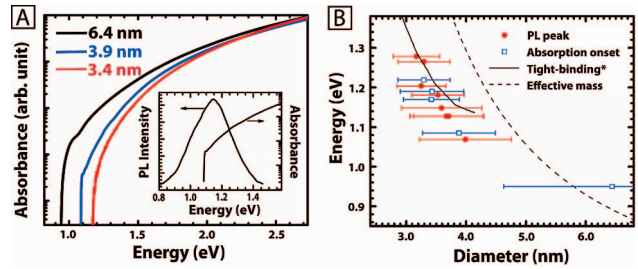

Figure 3. Size-dependent optical properties of ODE-capped Ge nanocrystals. (A) Absorbance spectra of Ge NCs with different average particle sizes. Log of absorbance is shown to highlight the relatively weak onset, due to the indirect-gap character of the Ge band-edge transition. Inset shows PL and absorption spectra taken from the 3.9 nm sample. (B) PL peak positions (solid) and absorption onsets (open) from solutions of Ge NCs of different particle sizes. Solid and dashed lines are taken from ref 21 and particle-in-a-box model, respectively.

Acknowledgment. This work was supported by the Chemical Science, Biosciences and Geosciences Division of the Office of Basic Energy Sciences, Office of Science, U.S. DOE, and by Los Alamos Laboratory Directed Research and Development funds. D.C.L. is a Los Alamos National Laboratory Director's Fellow. We thank Darrick J. Williams for performing X-ray diffraction.

Supporting Information Available: Experimental details, X-ray diffraction pattern, energy dispersive X-ray spectrum, PL spectrum that shows both visible and infrared emissions. This material is available free of charge via the Internet at http://pubs.acs.org.

References

(1) Canham, L. T. *Appl. Phys. Lett.* **1990**, *57*, 1046–1048.
(2) Takeoka, S.; Fujii, M.; Hayashi, S.; Yamamoto, K. *Phys. Rev. B* **1998**, *58*, 7921–7925.
(3) Nakamura, Y.; Watanabe, K.; Fukuzawa, Y.; Ichikawa, M. *Appl. Phys. Lett.* **2005**, *87*, 133119.
(4) Murray, C. B.; Norris, D. J.; Bawendi, M. G. *J. Am. Chem. Soc.* **1993**, *115*, 8706–8715.
(5) Murray, C. B.; Sun, S. H.; Gaschler, W.; Doyle, H.; Betley, T. A.; Kagan, C. R. *IBM J. Res. Dev* **2001**, *45*, 47–56.
(6) Micic, O. I.; Sprague, J. R.; Curtic, C. J.; Jones, K. M.; Machol, J. L.; Nozik, A. J.; Giessen, H.; Fluegel, B.; Mohs, G.; Peyghambarian, N. *J. Phys. Chem.* **1995**, *99*, 7754–7759.
(7) Wang, W.; Huang, J.; Ren, Z. *Langmuir* **2005**, *21*, 751–754.
(8) Taylor, B. R.; Kauzlarich, S. M.; Lee, H. W. H.; Delgado, G. R. *Chem. Mater.* **1998**, *10*, 22–24.
(9) Wilcoxon, J. P.; Provencio, P. P.; Samara, G. A. *Phys. Rev. B* **2001**, *64*, 035417.
(10) Gerung, H.; Bunge, S. D.; Boyle, T. J.; Brinker, C. J.; Han, S. M. *Chem. Commun.* **2005**, *2005*, 1914–1916.
(11) Heath, J. R.; Shiang, J. J.; Alivisatos, A. P. *J. Chem. Phys.* **1994**, *101*, 1607–1615.
(12) Lu, X. M.; Korgel, B. A.; Johnston, K. P. *Chem. Mater.* **2005**, *17*, 6479–6485.
(13) Gerion, D.; Zaitseva, N.; Saw, C.; Casula, M. F.; Fakra, S.; Van Buuren, T.; Galli, G. *Nano Lett.* **2004**, *4*, 597–602.
(14) Kornowski, A.; Giersig, M.; Vogel, R.; Chemseddine, A.; Weller, H. *Adv. Mater.* **1993**, *5*, 634–636.
(15) Hanrath, T.; Korgel, B. A. *J. Am. Chem. Soc.* **2004**, *126*, 15466–15472.
(16) Henderson, E. J.; Hessel, C. M.; Veinot, J. G. C. *J. Am. Chem. Soc.* **2008**, *130*, 3624–3632.
(17) Fuchs, R.; Moore, L. O.; Miles, D.; Gilman, H. *J. Org. Chem.* **1956**, *21*, 1113–1117.
(18) Buriak, J. M. *Chem. Rev.* **2002**, *102*, 1271–1308.
(19) Li, X.; He, Y.; Swihart, M. T. *Langmuir* **2004**, *20*, 4720–4727.
(20) Jurbergs, D.; Rogojina, E.; Mangolini, L.; Kortshagen, U. *Appl. Phys. Lett.* **2006**, *88*, 233116.
(21) Hill, N. A.; Pokrant, S.; Hill, A. J. *J. Phys. Chem. B* **1999**, *103*, 3156–3161.
(22) Hope-Weeks, L. J. *Chem. Lett.* **2005**, *34*, 1526–1527.
(23) Lu, X.; Ziegler, K. J.; Ghezelbash, A.; Johnston, K. P.; Korgel, B. A. *Nano Lett.* **2004**, *4*, 969–974.
(24) Zaitseva, N.; Dai, Z. R.; Grant, C. D.; Harper, J.; Saw, C. *Chem. Mater.* **2007**, *19*, 5174–5178.
(25) Zacharias, M.; Fauchet, P. M. *J. Non-Cryst. Solids* **1998**, *227−230*, 1058–1062.

JA809218S